Exchange Driven Growth

E. Ben-Naim[*]
Theoretical Division and Center for Nonlinear Studies,
Los Alamos National Laboratory, Los Alamos, New Mexico, 87545

P. L. Krapivsky[†]
Center for Polymer Studies, and Department of Physics, Boston University, Boston, MA, 02215

We study a class of growth processes in which clusters evolve via exchange of particles. We show that depending on the rate of exchange there are three possibilities: I) Growth: Clusters grow indefinitely; II) Gelation: All mass is transformed into an infinite gel in a finite time; and III) Instant Gelation. In regimes I and II, the cluster size distribution attains a self-similar form. The large size tail of the scaling distribution is $\Phi(x) \sim \exp(-x^{2-\nu})$, where ν is a homogeneity degree of the rate of exchange. At the borderline case $\nu = 2$, the distribution exhibits a generic algebraic tail, $\Phi(x) \sim x^{-5}$. In regime III, the gel nucleates immediately and consumes the entire system. For finite systems, the gelation time vanishes logarithmically, $T \sim [\ln N]^{-(\nu-2)}$, in the large system size limit $N \to \infty$. The theory is applied to coarsening in the infinite range Ising-Kawasaki model and in electrostatically driven granular layers.

PACS numbers: 05.40.-a, 05.20.Dd, 5.45.-a

I. INTRODUCTION

A multitude of growth phenomena in physical processes are driven by exchange of particles between clusters. Examples include droplet growth via evaporation and re-condensation [1], island growth in deposition processes [2], and phase ordering [3–5]. Exchange processes have been also used to model social and economical systems including segregation of heterogeneous populations [6], the distribution of wealth in a society [7], and growth of urban populations [8].

In exchange processes, clusters are composed of 'atoms' (monomers). Monomers detach from one cluster and reattach to another cluster. We shall consider the detachment controlled limit where the time scale for transport between clusters is much faster then the time scale for detachment. Exchange processes incorporate both reversible and irreversible features. Clusters may grow or shrink, yet when a monomer attaches to another cluster, its respective cluster disappears. This irreversible step provides the mechanism for cluster growth. Therefore, exchange-driven processes are fundamentally different from irreversible growth processes, particularly aggregation [9–12].

Such mass transfer processes are governed by an exchange kernel $K(i, j)$ that represents the rate of transfer of monomers from a cluster of size i to a cluster of size j. Generally, the rate of monomer exchange between two clusters depends on their sizes. Moreover, we consider the case where there is *no* preferable direction for exchanges, i.e., symmetric exchange kernels, $K(i, j) = K(j, i)$. This is unlike migration processes where the exchange is preferential ("big gets bigger" or "rich gets richer"). Migration underlies certain physical processes (e.g., coarsening with conserved order parameter [3, 4]) as well as social and economical processes [7, 8].

We investigate homogeneous exchange kernels, $K(ai, aj) = a^{2\lambda}K(i, j)$. In particular, we consider the product kernel $K(i, j) = (ij)^\lambda$ and its generalization $K(i, j) = i^\nu j^\mu + i^\mu j^\nu$ with $\nu + \mu = 2\lambda$ and $\nu \geq \mu$. We obtain a complete description of the problem in the asymptotic scaling regime. The overall range of possible behaviors and the emergence of self-similar size distributions are as in aggregation and migration processes. However, there are quantitative and qualitative differences. Unlike aggregation, the gelation transition is complete, and unlike migration, the size distributions are extended rather than compact.

We show that the behavior falls into three categories. I) Growth: When $\nu < 2$ and $\lambda < 3/2$, clusters grow indefinitely. The typical cluster size grows algebraically with time, $k \sim t^{1/(3-2\lambda)}$, and the cluster size distribution is given by a self-similar distribution with a stretched exponential tail. II) Gelation: When $\nu < 2$ and $\lambda > 3/2$, the entire mass in the system is suddenly transformed into an infinite gel at gelation time t_c. The cluster mass diverges algebraically near the gelation point, $k \sim (t_c - t)^{1/(3-2\lambda)}$, and a scaling behavior similar to the one underlying the growth phase is found. In the borderline case $\nu = 2$ the scaling function has an algebraic tail with a universal exponent $\Phi(x) \sim x^{-5}$. Scaling breaks down in the special point $\nu = \mu = 2$ where the distribution is log-normal. III) Instant gelation: When $\nu > 2$, the gelation time vanishes logarithmically with the system size, $t_c \sim [\ln N]^{-(\nu-2)}$. In particular, for an infinite system, gelation is instantaneous.

This paper is organized as follows. In the next section, we define the exchange process. The governing equations are analyzed using scaling techniques and exact solutions

[*]Electronic address: ebn@lanl.gov
[†]Electronic address: paulk@bu.edu

for the moments. We first analyze the product kernel (Sec. III) and then, the generalized kernel (Sec. IV). The gelation time in finite systems is investigated in Sec. V using heuristic arguments and numerical simulations. Applications to coarsening in the Ising model with infinite range Kawasaki dynamics and in electrostatically driven granular layers are briefly discussed in Sec. VI, and conclusions are given in Sec. VII.

II. EXCHANGE PROCESSES

We consider the following elementary exchange process. The system consists of an ensemble of clusters and clusters evolve via transfer of a single monomer from one cluster to another. Symbolically,

$$(i,j) \xrightarrow{K(i,j)} (i \pm 1, j \mp 1) \tag{1}$$

with i and j the number of particles in each cluster and $K(i,j)$ the exchange kernel. In an exchange event, a cluster is equally likely to gain or to lose a particle. Since the exchange process is unbiased, the matrix of transition rates is symmetric: $K(i,j) = K(j,i)$. Unbiased exchanged processes were studied in [7] and more systematically in Refs. [13, 14].

Let $A_k(t)$ be the density of clusters containing k monomers at time t. It evolves according to the following rate equation

$$\frac{dA_k}{dt} = \sum_{i,j} A_i A_j K(i,j) \left[\delta_{k,i+1} + \delta_{k,i-1} - 2\delta_{k,i}\right]. \tag{2}$$

This equation assumes perfect mixing, or equivalently, absence of spatial correlations. We restrict our attention to monodisperse initial conditions, $A_k(0) = \delta_{k,1}$. The exchange process has a single conservation law. As reflected by the evolution equations, the total mass is conserved, $M_1 = 1$ with $M_a = \sum_n k^a A_k(t)$ the moments of the size distribution. It is natural to consider homogeneous kernels, $K(ai, aj) = a^{2\lambda} K(i,j)$ with 2λ the homogeneity degree and we present results for the product kernel $K(i,j) = (ij)^\lambda$ and the generalized homogeneous kernel $K(i,j) = i^\nu j^\mu + i^\mu j^\nu$ with $\mu + \nu = 2\lambda$. The special case $\mu = 1$ was studied in ref. [13].

III. THE PRODUCT KERNEL

For the product kernel, $K(i,j) = (ij)^\lambda$, the rate equations (2) read

$$\frac{dA_k}{dt} = M_\lambda \left[(k+1)^\lambda A_{k+1} + (k-1)^\lambda A_{k-1} - 2k^\lambda A_k\right]$$

with the boundary condition $A_0 \equiv 0$. These evolution equations demonstrate the diffusive character of the exchange process. Absorbing the factor M_λ into the time variable

$$\tau = \int_0^t dt'\, M_\lambda(t') \tag{3}$$

we recast the governing equations into

$$\frac{dA_k}{d\tau} = (k+1)^\lambda A_{k+1} + (k-1)^\lambda A_{k-1} - 2k^\lambda A_k\,. \tag{4}$$

Alternatively, one can study integer moments of the size distribution. The total density obeys $\frac{d}{d\tau} M_0 = -A_1$, the total mass is conserved $\frac{d}{d\tau} M_1 = 0$, and higher integer moments satisfy the following hierarchy of equations

$$\frac{dM_n}{d\tau} = 2 \sum_{l=1}^{[n/2]} \binom{n}{2l} M_{n-2l+\lambda}. \tag{5}$$

Only for integer values of the homogeneity index is this hierarchy closed. We employ different approaches for different λ's. For $\lambda < 2$, we perform a scaling analysis of the rate equations and for $\lambda \geq 2$, we analyze the moment equations. This general analysis is augmented by exact solutions for the integer values $\lambda = 0$, 1, and 2.

A. Scaling ($\lambda < 2$)

When $\lambda < 2$, dimensional analysis of Eq. (4) shows that the typical cluster size grows as

$$k \sim \tau^\alpha, \qquad \text{with} \qquad \alpha = \frac{1}{2-\lambda}. \tag{6}$$

Using $\frac{d\tau}{dt} = M_\lambda \sim \tau^{\alpha(\lambda-1)}$, the growth of the typical scale is expressed in terms of the physical time

$$k \sim \begin{cases} t^\beta & \lambda < 3/2, \\ \exp(\text{const.} \times t) & \lambda = 3/2, \\ (t_c - t)^\beta & 3/2 < \lambda < 2. \end{cases} \tag{7}$$

The dynamical exponent is $\beta = (3-2\lambda)^{-1}$. As long as $\lambda < 3/2$, clusters grow indefinitely and the characteristic size grows algebraically with time. For $\lambda > 3/2$, a gelation transition occurs, i.e., the system develops a giant cluster in a finite time t_c.

We seek a scaling solution of the rate equations

$$A_k(\tau) \simeq \tau^{-2\alpha} \Phi\left(k\,\tau^{-\alpha}\right). \tag{8}$$

Mass conservation dictates the normalization $J_1 = 1$ where $J_a = \int dx\, x^a\, \Phi(x)$ is the a^{th} moment of the scaling distribution. Technically, the scaling function describes the behavior in the limits $k \to \infty$, $\tau \to \infty$ with the variable $x = k\tau^{-\alpha}$ fixed. Thus, we consider the continuum limit of the rate equation $\frac{\partial}{\partial\tau} A(k,\tau) = \frac{\partial^2}{\partial k^2}\left[k^\lambda A(k,\tau)\right]$. The scaling function satisfies the second order linear differential equation

$$(2-\lambda)\,\frac{d^2}{dx^2}\left[x^\lambda \Phi(x)\right] + x\frac{d}{dx}\Phi(x) + 2\Phi(x) = 0. \tag{9}$$

Multiplying this equation by x, employing the identities $x^2\Phi' + 2x\Phi = (x^2\Phi)'$, $x\Psi'' = (x\Psi)'' - 2\Psi'$, and integrating once yields $(2-\lambda)\left[(x^{\lambda+1}\Phi)' - 2x^\lambda\Phi\right] + x^2\Phi(x) = 0$. Integrating a second time gives the scaling function:

$$\Phi(x) = C\, x^{1-\lambda} \exp\left[-\frac{x^{2-\lambda}}{(2-\lambda)^2}\right] \tag{10}$$

with $C = (2-\lambda)^{-2/(2-\lambda)}/\Gamma\left(\frac{1}{2-\lambda}\right)$ found from the condition $J_1 = 1$. The nature of the scaling function differs from that found for migration where $K(l,m) = 0$ for $l < m$ [8]: Exchange is characterized by extended distributions, while migration is characterized by compact distributions.

There are two important cases [7, 13] for which the rate equations can be solved exactly. When the exchange kernel is independent of the cluster size ($\lambda = 0$), the rate equation is $\frac{d}{d\tau}A_k = A_{k+1} + A_{k-1} - 2A_k$ and the cluster size distribution is [7]

$$A_k = e^{-2\tau}\left[I_{k-1}(2\tau) - I_{k+1}(2\tau)\right], \tag{11}$$

where I_n is the modified Bessel function of order n [15]. In agreement with the general scaling analysis, the typical scale grows diffusively, $k \sim \tau^{1/2}$, and the scaling function is given by $\Phi(x) = (4\pi)^{-1/2}x\,\exp(-x^2/4)$.

For the pure product kernel ($\lambda = 1$), the rate equations read $\frac{d}{dt}A_k = (k+1)A_{k+1} + (k-1)A_{k-1} - 2kA_k$ (in this case $t = \tau$). Substituting the mass-conserving ansatz $A_k = (1-u)^2u^{k-1}$ reduces the infinite set of rate equations into a single ordinary differential equation $\frac{d}{dt}u = (1-u)^2$ subject the initial condition $u(0) = 0$. The size distribution in this case is [13]

$$A_k = \frac{t^{k-1}}{(1+t)^{k+1}}\,. \tag{12}$$

The typical cluster size grows ballistically, $k \sim t$, and the scaling function is purely exponential, $\Phi(x) = e^{-x}$, again in agreement with the above scaling results.

When $3/2 < \lambda < 2$, an infinite cluster is formed at some finite time t_c, termed the gelation time. The gelation time *depends* on the initial condition and its determination requires the full time dependent behavior. Even without knowing the gelation time exactly, one can describe the behavior in the pregel stage since the size distribution still admits the scaling form (10). Thus, for all $\lambda < 2$ we have

$$A_k(\tau) \simeq C\, k^{1-\lambda}\tau^{-\frac{3-\lambda}{2-\lambda}} \exp\left[-\frac{k^{2-\lambda}\,\tau^{-1}}{(2-\lambda)^2}\right]. \tag{13}$$

From this equation we see that $A_k \to 0$ in the limit $\tau \to \infty$ ($t \to t_c$). In other words, the gelation is complete at the gelation point: $A_k(t) = 0$ for $t \geq t_c$. This surprising behavior is akin to a first order phase transition. By contrast, gelation in aggregation processes [16, 17] is similar to a continuous transition – at the gelation point, the gel has an infinitesimal fraction of the entire mass, then the gel continuously grows and finite clusters disappear only when $t = \infty$.

Complete gelation can be alternatively shown as follows. Let us assume that the cluster size distribution approaches a constant $A_k \to A_k^* > 0$ as $\tau \to \infty$. From Eqs. (4), the quantities $B_k \equiv k^\lambda A_k^*$ satisfy the discrete Laplace equation $B_{k+1} + B_{k-1} - 2B_k = 0$ for $k > 1$ and $B_2 = 2B_1$. Solving recursively yields $B_k = kB_1 = kA_1^*$ or $A_k^* = k^{1-\lambda}A_1^*$. Mass conservation, $\sum_k kA_k^* = 1$, implies $A_1^* = 0$, and thence $A_k^* = 0$ for all k, i.e., complete gelation.

B. Multiscaling ($\lambda = 2$)

In this special case, the moment equations (5) are closed for $n \geq 2$. For example

$$\begin{aligned} \frac{dM_2}{d\tau} &= 2M_2, \\ \frac{dM_3}{d\tau} &= 6M_3, \\ \frac{dM_4}{d\tau} &= 12M_4 + 2M_2. \end{aligned} \tag{14}$$

The solutions to these equations are combinations of exponentials: $M_2 = e^{2\tau}$, $M_3 = e^{6\tau}$, $M_4 = \frac{6}{5}e^{12\tau} - \frac{1}{5}e^{2\tau}$, etc. The physical time $t = \frac{1}{2}[1 - e^{-2\tau}]$ is found from $t = \int_0^\tau ds M_2^{-1}(s)$ so

$$\begin{aligned} M_2 &= (1-2t)^{-1}, \\ M_3 &= (1-2t)^{-3}, \\ M_4 &= \frac{6}{5}(1-2t)^{-6} - \frac{1}{5}(1-2t)^{-1}. \end{aligned} \tag{15}$$

Therefore, the gelation time is $t_c = 1/2$. Asymptotically, the first term in (5) dominates: $\frac{d}{d\tau}M_n \simeq n(n-1)M_n$ implying $M_n \sim \exp[n(n-1)\tau]$ for $n > 1$. Close to the gelation time ($t \to t_c$), the moments diverge according to

$$M_n(t) \sim (t_c - t)^{-n(n-1)/2}. \tag{16}$$

Hence moments exhibit multiscaling asymptotic behavior, i.e., properly normalized moments $M_n^{1/n}/M_1$ diverge.

To determine the asymptotic form of the size distribution we treat k as a continuous variable. For $\lambda = 2$, Eq. (4) becomes $\frac{\partial}{\partial\tau}A_k = \frac{\partial^2}{\partial k^2}[k^2A_k]$. This equation is equidimensional in k [15] thereby suggesting use of the variable $\xi = \ln k$ instead of k. Making the transformation from $A_k(t)$ to $A(\xi,\tau)$ defined via $A_k dk = A(\xi)d\xi$, we recast above equation for $A_k(t)$ into the following constant coefficients diffusion-convection equation

$$\left(\frac{\partial}{\partial\tau} - \frac{\partial}{\partial\xi}\right)A(\xi,\tau) = \frac{\partial^2}{\partial\xi^2}A(\xi,\tau). \tag{17}$$

With the initial conditions $A(\xi,0) = \delta(\xi)$, the solution reads $A(\xi,\tau) = (4\pi\tau)^{-1/2}\exp[-(\xi+\tau)^2/(4\tau)]$. The original distribution $A_k = k^{-1}A(\xi)$ is log-normal

$$A_k(\tau) \simeq (4\pi\tau)^{-1/2}e^{-\tau/4}k^{-3/2}\exp\left[-\frac{(\ln k)^2}{4\tau}\right]. \tag{18}$$

Again, the distribution vanishes at the transition point, i.e., the gelation transition is complete. Moreover, the mass distribution is algebraic, $A_k(t) \sim M_0(t)\, k^{-3/2}$ for sufficiently small masses, $k \ll \sqrt{\ln \frac{1}{1-2t}}$. The total density vanishes quite slowly near the transition point

$$M_0(t) \sim (1-2t)^{1/8} \left(\ln \frac{1}{1-2t} \right)^{-1/2} . \qquad (19)$$

We note that the density follows a different law than the one characterizing higher than first moments (16).

The size distribution does not follow a scaling behavior asymptotically and the log-normal distribution is responsible for the multiscaling behavior (16) of the moments. This differs from aggregation processes where the moments diverge as $M_n(t) \propto (t_c - t)^{-\alpha_n}$ with the exponent α_n *linear* in n [16].

C. Instant Gelation ($\lambda > 2$)

Gelation is now instantaneous and complete, that is $A_k(t) = 0$ for all k when $t > 0$. To prove this assertion we assume the opposite and arrive at a contradiction. Our analysis follows the ingenious argument devised by van Dongen [17] in the context of aggregation processes.

The moments M_n with integer $n \geq 2$ evolve according to (5). The first term in the summation yields a lower bound for their growth rate

$$\frac{dM_n}{d\tau} \geq n(n-1) M_{n-2+\lambda} \geq n(n-1)(M_n)^{1+\Lambda} \qquad (20)$$

with $\Lambda = \frac{\lambda-2}{n-1}$. The second inequality follows from the Jensen's inequality as shown below. Consider the auxiliary functions $\mathcal{M}_n$, evolving according to

$$\frac{d\mathcal{M}_n}{d\tau} = n(n-1)(\mathcal{M}_n)^{1+\Lambda} . \qquad (21)$$

Solving this equation subject to the initial condition $\mathcal{M}_n(0) = 1$ yields $\mathcal{M}_n = [1 - n(\lambda-2)\tau]^{-1/\Lambda}$. Therefore, $\mathcal{M}_n \to \infty$ as $\tau \to \tau_n = [n(\lambda-2)]^{-1}$. Since $M_n \geq \mathcal{M}_n$, the moment M_n diverges at least at τ_n. The series of times τ_n set an upper bound for the gelation time τ_c since all moments should be finite for $\tau < \tau_c$. As $\tau_n \to 0$ when $n \to \infty$, we conclude that $\tau_c = 0$ and thence, the gelation time vanishes $t_c = 0$.

The inequality $M_{n-2+\lambda} \geq (M_n)^{1+\Lambda}$ with $\Lambda = \frac{\lambda-2}{n-1}$ is derived as follows. Let the parameters $p_j \geq 0$ satisfy $\sum_j p_j = 1$ and let $\Phi(x)$ be a convex function. A convex function satisfies the Jensen inequality

$$\sum_{j=1}^{\infty} p_j \Phi(x_j) \geq \Phi\bigg(\sum_{j=1}^{\infty} p_j x_j \bigg). \qquad (22)$$

First, we substitute the coefficients $p_j = jA_j$ (from mass conservation $\sum_j jA_j = 1$) and the convex function $\Phi(x) = x^{1+\Lambda}$ ($\Lambda > 0$ for $\lambda > 2$) into the Jensen inequality. Then, choosing $x_j = j^{n-1}$ and using the relations $\sum p_j x_j = \sum j^n A_j = M_n$ and $\sum p_j \Phi(x_j) = M_{n-2+\lambda}$ we indeed obtain the above inequality.

IV. GENERALIZED KERNELS

The rates $K(i,j)$ underlying exchange processes are typically homogeneous functions of i and j (at least for large i and j). We restrict ourselves to such kernels. Apart from the homogeneity degree 2λ, homogeneous kernels are characterized by an additional exponent ν defined through the asymptotic $K(1,j) \sim j^\nu$ as $j \gg 1$. For $i \ll j$ the exchange kernel scales as $K(i,j) = i^{2\lambda} K(1, j/i) \sim i^\mu j^\nu$ with $2\lambda = \nu + \mu$. Therefore, we consider a specific generalization of the product kernel that exhibits these homogeneity properties

$$K(i,j) = i^\nu j^\mu + i^\mu j^\nu . \qquad (23)$$

More precisely, the asymptotics $K(i,j) \sim i^\mu j^\nu$ occurs for $i \ll j$ if $\nu \geq \mu$; since the kernel is symmetric, we can assume that $\nu \geq \mu$ without loss of generality. We expect that the homogeneity indices govern the overall qualitative behavior (growth, gelation, instant gelation), while the precise form of the kernel controls quantitative characteristics such as the size distribution.

For this exchange kernel, the rate equations (2) become

$$\begin{aligned} \frac{dA_k}{dt} &= M_\mu \left[(k+1)^\nu A_{k+1} + (k-1)^\nu A_{k-1} - 2k^\nu A_k \right] \\ &+ M_\nu \left[(k+1)^\mu A_{k+1} + (k-1)^\mu A_{k-1} - 2k^\mu A_k \right] . \end{aligned}$$

The following generalization of the modified time variable

$$\tau = \int_0^t dt' \sqrt{M_\nu(t') M_\mu(t')} \qquad (24)$$

handles the two indices symmetrically. In terms of this time, the evolution equations are

$$\begin{aligned} \frac{dA_k}{d\tau} &= R \left[(k+1)^\nu A_{k+1} + (k-1)^\nu A_{k-1} - 2k^\nu A_k \right] \\ &+ R^{-1} \left[(k+1)^\mu A_{k+1} + (k-1)^\mu A_{k-1} - 2k^\mu A_k \right] , \end{aligned}$$

with $R = \sqrt{M_\mu / M_\nu}$. Of course, the dynamics conserve mass: $\frac{d}{d\tau} M_1 = 0$. Higher integer moments evolve according to

$$\frac{dM_n}{d\tau} = 2 \sum_{l=1}^{[n/2]} \binom{n}{2l} \left[R M_{n-2l+\nu} + R^{-1} M_{n-2l+\mu} \right] . \qquad (25)$$

When $\nu < 2$, the scaling analysis follows closely the product kernel case. The overall growth laws (6) and (7) remain unchanged and the homogeneity degree λ characterizes the scaling behavior. However, we shall see that the individual indices ν and μ play an important role since they dictate the range for which this law holds.

We seek a scaling solution of the form (8). The scaling function $\Phi(x)$ satisfies

$$\frac{d^2}{dx^2}\Big[\big(Ux^\nu+Vx^\mu\big)\Phi(x)\Big]+x\,\frac{d}{dx}\Phi(x)+2\Phi(x)=0 \quad (26)$$

with the constants $U=\alpha^{-1}A$ and $V=\alpha^{-1}A^{-1}$ determined from the ratio $A=\sqrt{J_\mu/J_\nu}$. The scaling function reads

$$\Phi(x)=C\,\frac{x}{Ux^\nu+Vx^\mu}\,\exp\left[-\int_0^x dy\,\frac{y}{Uy^\nu+Vy^\mu}\right]. \quad (27)$$

The scaling solution involves three parameters U, V, and C. Substituting $U=\alpha^{-1}A$ and $V=\alpha^{-1}A^{-1}$ into the equality $A=\sqrt{J_\mu/J_\nu}$ yields a closed equation for the parameter A. Once A is determined, the parameters U and V follow, and finally, the amplitude C is found from the normalization $J_1=1$.

We now illustrate this procedure for the special case $(\nu,\mu)=(1,0)$, i.e., for the pure sum kernel $K(i,j)=i+j$. In this case, the integral on the right-hand side of Eq. (27) is readily computed. Using $U=\frac{3A}{2}$ and $V=\frac{3}{2A}$ we arrive at

$$\Phi(x)=C\,x\left(1+A^2x\right)^{a-1}\exp\left[-aA^2x\right] \quad (28)$$

with $a=\frac{2}{3}A^{-3}$. Substituting (28) into the right-hand side of the equality $A=\sqrt{J_0/J_1}$ transforms it into the equation $(\frac{e}{a})^a\,\Gamma(a,a)+a^{-1}=1$, involving the incomplete gamma function (see Appendix A). The amplitude is then explicitly evaluated to give $C=aA^6$. From the above transcendental equation we find $a\cong 2.82649$, and hence $A\cong 0.428397$, $C\cong 0.0174713$. Interestingly, there is a nontrivial algebraic correction to the leading exponential behavior, $\Phi(x)\sim x^a\exp(-aAx)$ for large x [18].

On the boundary $\nu=2$ separating regime III from the two other regimes, the solution of Eq. (27) significantly simplifies. We find $A=1/[2(2-\mu)]$, $U=1/4$, and $V=1/(2-\mu)^2$; consequently, the scaling function is

$$\Phi(x)=C\,x^{1-\mu}\left[1+\frac{x^{2-\mu}}{4(2-\mu)^2}\right]^{-1-\frac{4}{2-\mu}}. \quad (29)$$

The constant $C=2\left[2(2-\mu)\right]^{-1-\frac{2}{2-\mu}}\,\left[B(\frac{1}{2-\mu},\frac{3}{2-\mu})\right]^{-1}$ is expressed in terms of the beta function. Remarkably, the scaling function (29) exhibits a universal large-x asymptotic behavior

$$\Phi(x)\sim x^{-5}\,. \quad (30)$$

Hence the size distribution is algebraic, $A_k(\tau)\sim\tau^{3\alpha}\,k^{-5}$, with $\alpha=(2-\lambda)^{-1}=2/(2-\mu)$. With this algebraic divergence, sufficiently small moments are characterized by ordinary scaling behavior while higher moments exhibit multiscaling behavior:

$$M_n\sim\begin{cases}\tau^{\alpha(n-1)} & n<4,\\ \tau^{\alpha n(n-1)/4} & n>4.\end{cases} \quad (31)$$

This behavior follows from the leading term in the moment equation (25), viz. $\frac{d}{d\tau}M_n=n(n-1)M_nR$. With $R=\sqrt{M_\mu/M_2}\simeq A\tau^{-1}$ and $A=\alpha/4$, this equation becomes $\frac{d}{d\tau}M_n=\frac{\alpha n(n-1)}{4\tau}\,M_n$, leading to the multiscaling behavior (31).

The determination of A in the general situation requires numerical evaluation, yet the form and nature of the size distribution is clear. For example, the minimal (maximal) index governs the distribution of small (large) clusters. Indeed, from Eq. (27), the extremal behaviors are

$$\Phi(x)\sim\begin{cases}x^{1-\mu} & x\ll 1,\\ \exp[-x^{2-\nu}] & x\gg 1.\end{cases} \quad (32)$$

Apart from the point $(\nu,\mu)=(2,2)$, the scaling solution holds for all other $\mu<2$. As in the product kernel case, growth occurs when $\lambda<3/2$ and gelation occurs when $3/2<\lambda<2$.

For $\nu>2$, the scaling solution (27) predicts $\Phi\sim x^{1-\nu}$ for large x. Such behavior is inconsistent since the moment J_ν diverges and instead, instantaneous gelation occurs. The moments M_n with $n>1$ satisfy Eq. (25) and the first term in the summation yields a lower bound for the moment growth $\frac{d}{d\tau}M_n\geq Rn(n-1)M_{n-2+\nu}$. Keeping only this term and absorbing the factor R into the time variable, the previous proof applies. Thus, gelation is instantaneous.

Instant gelation arises when $\nu>2$, so it does not happen if for instance the exchange rate grows no faster than the mass, $\nu\leq 1$ (this condition is satisfied for the exchange processes discussed below in Sec. VI). In some situations, however, the condition $\nu\leq 1$ may be violated. We merely mention that in aggregation — processes realized via collisions and thus with rates whose growth is more restricted than in exchange — kernels with $\nu>1$ do appear in several applications ranging from the coalescence of raindrops [19–21] to the coalescence of planetesimals into planets [22] and stars into black holes [23].

To summarize, there are 3 types of behaviors, determined by the homogeneity degrees μ and ν (Fig. 1):

- I *Growth.* The cluster size grows indefinitely, and the size distribution obeys scaling.
- II *Gelation.* The cluster size diverges in a finite time and the size distribution follows a scaling solution near the gelation time. Gelation is complete.
- III *Instant Gelation.* The cluster size distribution vanishes for all $t>0$.

The cluster size distribution exhibits a scaling behavior in regimes I and II. Scaling behavior underlies the system everywhere except for regime III and the point $(2,2)$. In the bulk of regimes I and II the size distribution is a stretched exponential, while in the boundary with region III, the cluster size distribution has an algebraic tail. Last, at the point $(\mu,\nu)=(2,2)$ scaling breaks down and the distribution is log-normal.

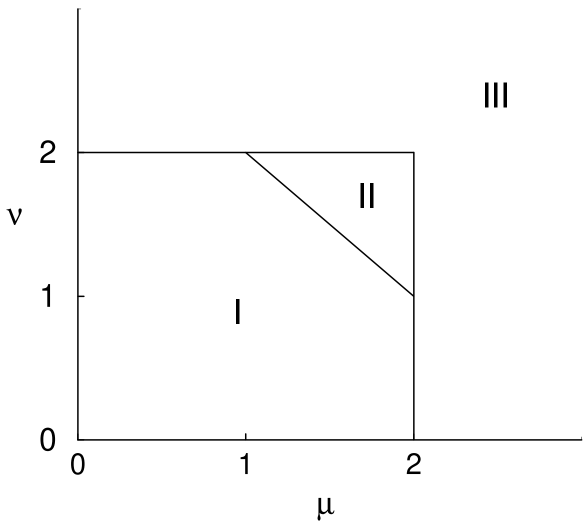

FIG. 1: The three types of behaviors: Scaling (I), Ordinary gelation (II), and Instant gelation (III).

V. THE GELATION TIME

Instantaneous gelation is certainly counter intuitive: A finite time singularity that occurs at time $t = +0$! Instantaneous gelation was investigated exclusively in the context of aggregation [12, 17, 24–28]. For infinite systems, it is impossible to quantify the difference between two instant gelling systems. Finite systems, on the other hand, naturally quantify how fast a system gels.

Consider a system consisting initially of N monomers. In a finite time t_N, all mass in the system condenses into a single 'runaway' cluster. How does the average gelation time $T_N = \langle t_N \rangle$ depend on N? When growth or ordinary gelation occurs, the answer follows from our previous analysis. In the scaling regime, the growth law (7) indicates that the condensation time grows algebraically with the system size, $T_N \sim N^{1/\beta}$. In the case of ordinary gelation, the average gelation time saturates at an N-independent value: $T_N \to t_c$. The interesting case is instant gelation where the gelation time vanishes in the thermodynamic limit, $T_N \to 0$ as $N \to \infty$.

For simplicity, we discuss the product kernel. The vanishing gelation time is ultimately related to the short time behavior. Early on, loss terms in the rate equation (4) are negligible and to leading order $\frac{d}{dt} A_j \cong (j+1)^\lambda A_{j+1}$, where we tacitly assumed $\tau \equiv t$. For the initial condition $A_j(0) = \delta_{j,1}$, the leading order behavior of the density is

$$A_{j+1} \cong (j!)^{\lambda-1}\, t^j. \tag{33}$$

In a finite system consisting initially of N monomers, a j-mer first appears at time $t_j \approx (j!)^{-(\lambda-1)/j} N^{-1/j}$, estimated from $NA_j(t_j) = 1$. For example, the first dimer and trimer appear at times $t_2 = N^{-1}$ and $t_3 = 2^{-(\lambda-1)/2} N^{-1/2}$, respectively. By definition, the times increase monotonically, $t_{j+1} > t_j$, yet the above estimates increase monotonically only for sufficiently small $j < j_*$. From $t_{j_*} = t_{j_*+1}$, we obtain the extremum $j_* = (\lambda-1)^{-1} \ln N$ using the Stirling formula. The corresponding time $T_* \equiv t_{j_*}$ is

$$T_* \sim \left(\frac{\lambda-1}{\ln N}\right)^{\lambda-1}. \tag{34}$$

For later times, $t \gg T_*$, the rate equations should be modified to account for the finiteness of the system (see e.g. [29, 30]) since significant statistical fluctuations are induced by large runaway clusters that take over (eventually only one such cluster remains). The critical size of such clusters is $j_* \sim (\lambda-1)^{-1} \ln N$. As a complete analytical solution seems out of reach, we proceed heuristically by focusing on the leading cluster that eventually grows to be the gel. Since it exchanges monomers back and forth with other clusters its growth mechanism is diffusive. For an ordinary diffusive process, $\frac{d}{dt}\langle k \rangle = 0$, while $\frac{d}{dt}\langle k^2 \rangle = D$. In our case, $D = k^\lambda$ with the typical size $k^2 \equiv \langle k^2 \rangle$. Therefore, the typical size of the runaway cluster grows according to

$$\frac{dk}{dt} = k^{\lambda-1}. \tag{35}$$

Integrating this rate equation from the critical size $k = j_*$ to the system size $k = N$ gives the gelation time

$$T_N = T_* + \frac{1}{\lambda-2}\left[\frac{1}{j_*^{\lambda-2}} - \frac{1}{N^{\lambda-2}}\right]. \tag{36}$$

Since $j_* = (\lambda-1)^{-1} \ln N$, the duration of the latter growth phase is much larger than that of the nucleation phase, $T_N \gg T_*$. Therefore, the gelation time vanishes logarithmically

$$T_N \sim (\ln N)^{-(\lambda-2)}, \tag{37}$$

in the thermodynamic limit. A straightforward extension of the above argument to the generalized exchange kernel (23) gives $T_N \sim (\ln N)^{-(\nu-2)}$.

Therefore, in a finite system it may be difficult to distinguish instantaneous gelation from the ordinary one. We verified the logarithmic law (37) numerically for $\lambda = 3$ (Fig. 2). To probe fluctuations in the gelation time, we examined the variance. We observed that the normalized variance $\sigma_N^2 = \langle t_N^2 \rangle / \langle t_N \rangle^2 - 1$ vanishes logarithmically in the thermodynamic limit (Fig. 2). The distribution of normalized gelation times becomes trivial $P(t_N/T_N) \to \delta(z-1)$ implying that the gelation time is a self-averaging quantity.

We also examined the gelation time in two other growth processes, namely aggregation [9–11] and addition [31, 32]. The above heuristic picture yields a similar logarithmic law albeit with a different exponent [28]. Self-averaging is observed numerically as well, and we conclude that the behavior found for exchange processes is generic.

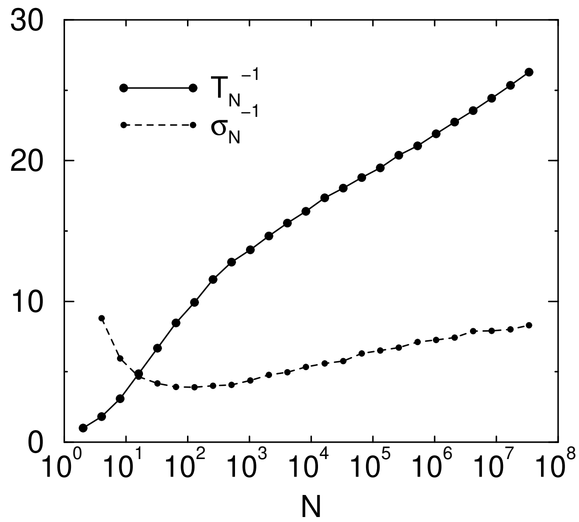

FIG. 2: The system size dependence of the gelation time. Shown are the average gelation time T_N and the normalized variance σ_N versus the system size. The Monte Carlo simulation results correspond to an average over 10^3 independent realizations of the exchange process with $\lambda = 3$.

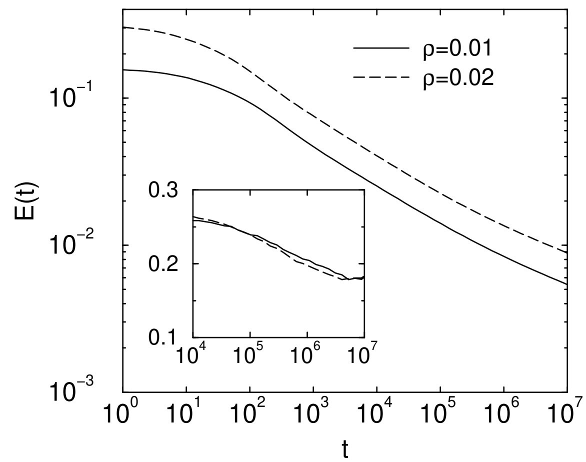

FIG. 3: Decay of the energy versus time in the Ising-Kawasaki model with infinite range exchange. The inset shows the local slope $-d\ln E(t)/d\ln t$ versus time t.

VI. APPLICATIONS TO COARSENING

In exchange processes, a monomer detaches from a cluster and subsequently re-attaches to another cluster. This elementary mechanism underlies a number of growth and coarsening processes. We apply our general theory to two coarsening processes.

A. Infinite range Ising-Kawasaki model

Consider the model proposed by Schelling [6] that mimics segregation in initially homogeneous systems. In its simplest version, the segregation model is defined on a lattice completely filled by two species. Any two dissimilar particles can exchange locations if this move does not increase the total number of broken bonds (dissimilar nearest neighbors). This model is essentially the Ising model with Kawasaki zero-temperature spin exchange dynamics [33–35]. In contrast with the usual local (typically nearest-neighbor) exchanges, exchange in the segregation model is non-local. This process is still not a mean-field one as broken bonds are counted locally.

To appreciate the difference between the nearest-neighbor and infinite range *zero-temperature* Kawasaki dynamics recall that subject to local exchange, the Ising system freezes. This is obvious in one dimension where a string of alternating domains each of length ≥ 2 could not further evolve and it remains true in higher dimensions [36]. By contrast, the Ising model with infinite range zero-temperature Kawasaki dynamics coarsens. In one dimension, the domain size distribution can be obtained analytically [37]. The situation in higher dimensions is an open question [33–35].

We considered the limit of a *vanishing* fraction of one of the two phases. While interesting on its own, this case is also relevant to sociological applications. In this limit, domains of the minority phase are isolated and the process is essentially an exchange process with a product kernel $K(i,j) = (ij)^\lambda$. The dependence of the number of exchange candidates (i.e., spins in domain walls that can lower their energy by hoping to a different cluster) on the cluster size dictates the homogeneity degree. For spherical clusters, only perimeter spins may exchange. Since the island size and the surface size grow with the radius according to $k \sim R^d$ and $\sigma \sim R^{d-1} \sim k^{(d-1)/d}$, respectively, one has $\lambda = (d-1)/d$. Hence $\beta = d/(d+2)$ [recall that the exponent β is defined via $k \sim t^\beta$ and equal to $\beta = 1/(3-2\lambda)$, Eq. (7)]. The dynamical exponent (defined through $R \sim t^z$) is therefore $z = 1/(d+2)$. If the islands are polygons, a distinct possibility on a lattice, then only corner spins are active so $\lambda = 0$, and consequently $\beta = 1/3$ and $z = 1/(3d)$. Both estimates agree with the exact result in one dimension [37].

To examine these predictions, we performed large scale Mote Carlo simulations of the Ising model with infinite range Kawasaki exchange dynamics in two dimensions. The efficient simulation method keeps track only of boundary spins. The simulation data in Fig. 3 corresponds to an average over 10^2 independent realizations in a square lattice of 6000×6000 sites with minority spin concentrations of $\rho = 0.01$ and 0.02. The density of broken bonds (i.e., the energy) $E(t)$ provides a convenient measure for the domain growth law. If n is the density of minority domains, then conservation of the total number of minority spins gives $nR^d \sim$ const, and using compactness of the domains we get $E \sim nR^{d-1}$ from which $E \sim R^{-1} \sim t^{-z}$. Our numerical simulations show a very slow growth law for the typical domain size. The simulations exclude the former circular domain sce-

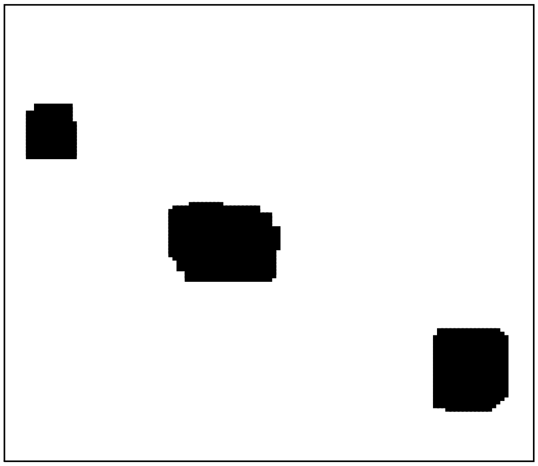

FIG. 4: A snapshot of a small part of the system at the late stage of evolution ($t = 10^6$).

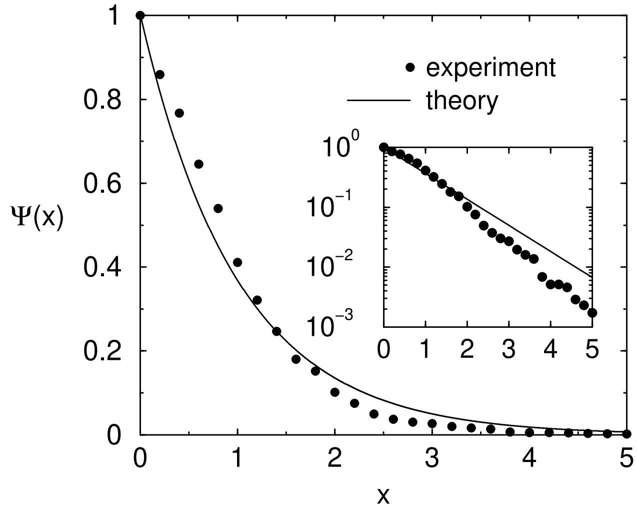

FIG. 5: The cumulative cluster area distribution $\Psi(x)$ versus the normalized area x. The inset magnifies the tail of the distribution (same axis labels as the main figure).

nario $z = 1/(d+2) = 1/4$ and give support to the latter square domain scenario $z = 1/(2d) = 1/6$. Additionally, we verified that the shape of the domains is not circular, but rather close to rectangular with a mostly straight edges (Fig. 4). Thus, the growth may not necessarily follow from curvature considerations. We conclude that the growth law is dimension dependent, at least in the limit of *vanishing* minority concentration.

B. Coarsening of thin granular layers

In electrostatically driven granular layers, clusters nucleate around large grains [38]. When charged grains oscillate back and forth between the two bounding plates due to the oscillating electric field, they may scatter of the plate or collide with other particles. Consequently, individual grains may transfer from one cluster to another. Naively, the rate of hoping into and out of a cluster is proportional to its area. Therefore, the homogeneity degree is unity, $\lambda = 1$, implying $\beta = 1$ and a dynamical exponent of $z = 1/d$. In two dimensions, this prediction is consistent with the experimental observation $z = 1/2$ [38].

To further test the exchange driven growth theoretical predictions, we examined the experimentally observed cluster size distributions. First, we checked that the size distributions at different times are identical once the average cluster size is set to unity, thereby verifying the self-similar behavior. Given the relatively small number of available clusters, experimental data from different stages during the coarsening process were aggregated into a single data set by setting the average cluster size (or area) to unity. To further improve the statistics, we examined the cumulative size distribution, $\Psi(x) = \int_x^\infty dy\, \Phi(y)$. The theory (12) predicts a purely exponential distribution, $\Psi(x) = \Phi(x) = \exp(-x)$. The experimental distribution represents roughly 10^3 clusters obtained from 20 different snapshots during a single realization of the coarsening process in which the total number of clusters decreased appreciably from 200 to 10.

Comparing the theoretical and experimental size distributions, exchange driven growth provides a useful approximation (see Fig. 5). For instance, the normalized variance, defined via $\sigma^2 = J_2/J_1^2 - 1$, is experimentally found to be $\sigma = 0.80 \pm 0.05$ compared with the theoretical value $\sigma = 1$. Although exchange of individual grain does underlie the experimental coarsening process, the exchange usually involves only neighboring clusters. Thus, the mean-field exchange driven growth process where exchange can occur between any two clusters is only an approximation. Further, more extensive experimental data is needed to resolve the relevance of spatial correlations.

VII. CONCLUSIONS

We have shown that kinetics of exchange processes are classified by the homogeneity indices of the governing rates. There are three possible regimes including indefinite growth, gelation in a finite time, and instant gelation. Scaling behavior underlies the first two regimes. The size distributions are generally extended, decaying exponentially or algebraically for large sizes, in contrast with migration processes.

We also studied the gelation time in finite systems and found that it decays rather slowly, following an inverse logarithmic law. It would be interesting to determine further temporal characteristics in the instant gelation regime [28]. While instant gelation may seem unphysical, there is no obvious restriction on the homogeneity indices that forbids instant gelation. The finite system size or physical restrictions on the aggregate sizes may cause a system that technically is in the instant gelation regime to gel only in a finite time and therefore characterization of the instant gelation regime may still be practically relevant.

Our description was on a mean-field level where all pairs of clusters in the system are equally likely to interact. It will be interesting to incorporate spatial fluctuations into this description. The nature of the spatial fluctuations depends on the mechanism for transporting monomers from one cluster to the other. For diffusive transport, one can incorporate effective fluxes into clusters, using the standard techniques developed for reaction-diffusion processes.

Acknowledgments

We thank Igor Aronson and Avner Peleg for useful discussions. We are grateful to Igor Aronson for providing the experimental data. This research was supported by DOE (W-7405-ENG-36).

[1] P. Meakin, *Fractals, Scaling and Growth Far From Equilibrium* (Cambridge University Press, New York 1998).
[2] A. Zangwill, *Physics at Surfaces* (Cambridge University Press, New York 1988).
[3] I. M. Lifshitz and V. V. Slyozov, Zh. Eksp. Teor. Fiz. **35**, 479 (1959) [Sov. Phys. JETP **8**, 331 (1959)]; J. Phys. Chem. Solids **19**, 35 (1961).
[4] A. J. Bray, Adv. Phys. **43**, 357 (1994).
[5] C. Sire and S. N. Majumdar, Phys. Rev. E **52**, 244 (1995).
[6] T. Schelling, J. Math. Sociology **1**, 61 (1971).
[7] S. Ispolatov , P. L. Krapivsky, and S. Redner, Eur. Phys. J. B **2**, 267 (1998).
[8] F. Leyvraz and S. Redner, Phys. Rev. Lett. **88**, 068301 (2002).
[9] M. V. Smoluchowski, Z. Phys. Chem. **92**, 215 (1917).
[10] S. Chandrasekhar, Rev. Mod. Phys. **15**, 1 (1943).
[11] S. K. Frielander, *Smoke, Dust and Haze: Fundamentals of Aerosol Behavior* (Wiley, New York, 1977).
[12] For a recent review, see F. Leyvraz, Phys. Report, in press (2003).
[13] J. Ke and Z. Lin, Phys. Rev. E **66**, 050012 (2002).
[14] J. Ke and Z. Lin, Phys. Rev. E **67**, 031103 (2003).
[15] C. M. Bender and S. A. Orszag, *Advanced Mathematical Methods for Scientists and Engineers* (McGraw-Hill, New York, 1978).
[16] P. G. J. van Dongen and M. H. Ernst, Phys. Rev. Lett. **54**, 1396 (1985).
[17] P. G. J. van Dongen, J. Phys. A **20**, 1889 (1987).
[18] The scaling solution (28) disagrees with the purely exponential scaling distribution found in Ref. [13]. For $\mu \neq \nu$, the rate equations in [13] are inconsistent with a symmetric exchange kernel.
[19] H. Pruppacher and J. Klett, *Microphysics of Clouds and Precipitations* (Kluwer, Dordrecht, 1998).
[20] M. Pinsky, A. Khain, and M. Shapiro, J. Atmos. Sci. **58**, 742 (2001).
[21] G. Falkovich, A. Fouxon, and M. G. Stepanov, Nature **419**, 151 (2002).
[22] E. Kokubo and S. Ida, Icarus **123**, 180 (1996).
[23] M. H. Lee, Astrophys. J. **418**, 147 (1993).
[24] E. R. Domilovskii, A. A. Lushnikov, and V. N. Piskunov, Dokl. Phys. Chem. **240**, 108 (1978).
[25] E. M. Hendriks, M. H. Ernst, and R. M. Ziff, J. Stat. Phys. **31**, 519 (1983).
[26] J. L. Spouge, J. Colloid Inter. Sci. **107**, 38 (1985).
[27] I. Jeon, J. Stat. Phys. **96**, 1049 (1999).
[28] L. Malyushkin and J. Goodman, Icarus **150**, 314 (2001).
[29] A. A. Lushnikov, J. Colloid Inter. Sci. **65**, 276 (1977).
[30] H. Tanaka and K. Nakazawa, Icarus **107**, 404 (1994).
[31] N. V. Brilliantov and P. L. Krapivsky, J. Phys. A **24**, 4789 (1991).
[32] Ph. Laurençot, Nonlinearity **12**, 229 (1999).
[33] K. Kawasaki, Phys. Rev. **145**, 224 (1966).
[34] P. Tamayo and W. Klein, Phys. Rev. Lett. **63**, 2757 (1989).
[35] J. F. Annett and J. R. Banavar, Phys. Rev. Lett. **68**, 2941 (1992).
[36] A. Levy, S. Reich, and P. Meakin, Phys. Lett. A **87**, 248 (1982); P. Meakin and S. Reich, Phys. Lett. A **92**, 247 (1982); A. Sadiq and K. Binder, J. Stat. Phys. **35**, 517 (1984).
[37] E. Ben-Naim and P. L. Krapivsky, in preparation.
[38] I. Aranson, D. Blair, V. A. Kalatsky, G. W. Crabtree, W.-K. Kwok, V. M. Vinokur, and U. Welp, Phys. Rev. Lett. **84**, 3306 (2000).

APPENDIX A: THE CASE $(\nu,\mu)=(1,0)$

Substituting Eq. (28) into $A^2 = J_0/J_1$ yields

$$1 \;=\; \frac{\int_0^\infty dx\,x^2\,(1+x)^{b-1}\,e^{-ax}}{\int_0^\infty dx\,x\,(1+x)^{b-1}\,e^{-ax}}$$

with $b=a$. Evaluation of the ratio of the integrals is performed as follows

$$\begin{aligned}
1 &= -\frac{d}{da}\ln\left[\int_0^\infty dx\,x\,(1+x)^{b-1}\,e^{-ax}\right]\Big|_{a=b}\\
&= -\frac{d}{da}\ln\left[-\frac{d}{da}\left(\int_0^\infty dx\,(1+x)^{b-1}\,e^{-ax}\right)\right]\Big|_{a=b}\\
&= -\frac{d}{da}\ln\left[-\frac{d}{da}\left(e^a a^{-b}\,\Gamma(b,a)\right)\right]\Big|_{a=b}\\
&= \frac{a^{-2}+e^a a^{-a-1}\,\Gamma(a,a)}{a^{-1}}.
\end{aligned}$$